Saudi Journal of Biological Sciences 28 (2021) 6556–6567

Contents lists available at ScienceDirect

Saudi Journal of Biological Sciences

journal homepage: www.sciencedirect.com

Original article

Assessing the effect of human dental pulp mesenchymal stem cell secretome on human oral, breast, and melanoma cancer cell lines

A. Thirumal Raj [a], Supriya Kheur [a,*], Ramesh Bhonde [b], Vishnu R Mani [c], Hosam Ali Baeshen [d], Shankargouda Patil [e,*]

[a] Department of Oral Pathology and Microbiology, Dr.D.Y.Patil Dental College and Hospital, Dr.D.Y.Patil Vidyapeeth, Pune, India
[b] Dr.D.Y.Patil Vidyapeeth, Pune, India
[c] Division of Trauma, Acute and Critical Care Surgery, Department of Surgery, Johns Hopkins University School of Medicine, Baltimore, Maryland, The United States of America.
[d] Department of Orthodontics, College of Dentistry, King Abdulaziz University, Jeddah, Saudi Arabia
[e] Department of Maxillofacial Surgery and Diagnostic Sciences, Division of Oral Pathology, College of Dentistry, Jazan University, Jazan, Saudi Arabia

ARTICLE INFO

Article history:
Received 16 June 2021
Revised 25 June 2021
Accepted 6 July 2021
Available online 14 July 2021

Keywords:
Breast cancer
Conditioned media
Cytokines
Dental pulp
Growth factors
Melanoma
Mesenchymal stem cells
Oral cancer
Secretome

ABSTRACT

Background: The secretome of the dental pulp mesenchymal stem cells (DPMSCS-S) have an array of regenerative potential and could aid in the rehabilitation of cancer patients post-therapeutic interventions, although caution is required as DPMSC-S have shown to augment prostate cancer cells. Thus, it is vital to assess if these pro-carcinogenic effects extend to other cancer types.
Objective: To assess if DPMSC-S has any pro-carcinogenic effect on oral cancer, breast cancer, and melanoma cell lines.
Materials and methods: Conditioned media obtained from the isolated and characterized DPMSC (DPMSC-CM) were profiled using bead-based multiplex assay. AW13515 (oral cancer), MDA-MB-231 (breast cancer), and A-375 (melanoma) cell lines were exposed to 20%, 50%, and 100% DPMSC-CM for 24, 48, and 72 h. DPMSC-CM effect on the cancer cell properties and secretome were assessed.
Results: DPMSC-CM augmented invasion, adhesion, multi-drug resistance, DNA repair, and mitochondrial repair in AW13516 through upregulation of growth factors Ang-2, EGF, M−CSF, PDGF-AA, PDGF-BB, pro-inflammatory cytokines TNF-α, IL-2, downregulation of anti-inflammatory cytokine TGF-β1, and pro-inflammatory cytokine IL-4. In MDA-MB-231, invasion, and multi-drug resistance were augmented through upregulation of growth factors EGF, EPO, G-CSF, HGF, M−CSF, PDGF-AA, and pro-inflammatory cytokine TNF-α, CXCL10, IL-12p70. EMT, invasion, migration, and adhesion were augmented in A-375 through upregulation of growth factors Ang-2, EGF, PDGF-BB, TGF-α, pro-inflammatory cytokines TNF-α, and IL-17A.
Conclusion: DPMSC-CM can augment the carcinogenic properties of oral cancer, breast cancer, and melanoma cells, further animal model studies are required to validate our in-vitro findings.

1. Introduction

Mesenchymal stem cells (MSC) are emerging as an attractive and promising therapeutic avenue in numerous disease states including post-cancer treatment rehabilitation. The ongoing translational interest stems from some of their exclusive properties like multipotency, expression of specific cell surface antigen (Dominici et al., 2006), adherence to plastic surfaces, potential to differentiate into adipo-, osteo- and chondrogenic lineages among others (Horwitz et al., 2005). The above properties along with their role in the inflammatory milieu and complex interaction with host immune cells unfurled their immunomodulatory and regenerative potential. Their capacity to migrate and home to sites of injury

* Corresponding authors.
E-mail addresses: thirumalraj666@gmail.com (A.T. Raj), supriya.kheur@dpu.edu.in (S. Kheur), rrbhonde@gmail.com (R. Bhonde), vishnu.mani@duke.edu (V.R Mani), drbaeshen@me.com (H.A. Baeshen), dr.ravipatil@gmail.com (S. Patil).
Peer review under responsibility of King Saud University.

Production and hosting by Elsevier

https://doi.org/10.1016/j.sjbs.2021.07.029
1319-562X/

(Marofi et al., 2017) and aberration (neoplastic sites) via chemokine and soluble molecular factors have rendered profound interest in their potential as a carrier vehicle for drugs or genes. The rapid advances resulting in the application of MSC in regenerative medicine have further piqued and delineated the growth factors and cytokines from its secretome to be the primary effector. This has evolved into a cell-free therapy in tissue regeneration. Recent in-vitro and in-vivo animal model studies have deciphered and utilized MSC-derived secretome (MSC-S) to regenerate tissues, enhance wound healing, and ameliorate radiation-induced fibrosis (Aryan et al., 2018; Chen et al., 2018; Gunawardena et al., 2019; L et al., 2019).

In-vitro and in-vivo animal model studies on MSC derived from the oral cavity have been encouraging with gingiva MSC-S (GMSC-S) attenuating carcinogenesis in oral cancer cell lines (Ji et al., 2016). However, there are no studies to date investigating the role of DPMSC in the context of carcinogenesis except Dogan et al exploring the role of DPMSC in prostate cancer cell lines (Doğan et al., 2017). We questioned the pragmatic nature of the previous study as DPMSC is being actively sorted out by industry to translate their niche of regenerative properties for regeneration of maxillofacial skeleton, especially alveolar regeneration (Nakajima et al., 2018), and dental implant osteointegration (Irastorza et al., 2019). MSC has also shown the ability to enhance wound healing (Barbier et al., 2018) and possess anti-fibrotic effects (Iwanaka et al., 2020) which is a translatable application in oral fibrotic diseases such as oral sub-mucous fibrosis (Kheur et al., 2020). If proven, it is possible to extend DPMSC application to ameliorating radiation-induced fibrosis of cancer patients.

Hence in light of high clinical relevance and non-existent research in the specific field, we investigated to see if DPMSCS had any role in potentiating carcinogenesis among oral cancer, melanoma, and breast cancer cells consistent with the practical utility of these cell lines as described above. Our preliminary investigation indicated augmentation of several carcinogenic properties of the cancer cell line with DPMSC and we speculated that these effects are secondary to their secretome. Hence we performed series of experiments that unveiled DPMSC having a dual effect and upregulated carcinogenesis on all 3 cancer cell lines primarily through signaling from soluble factors in the secretome. These data suggest that there is an urgent need to investigate the in-vivo effects of DPMSC to mitigate any untoward harm and ensure patient safety.

2. Materials and methods

In-vitro cell culture and flow cytometry analysis: Institutional ethics review committee of Dr.D.Y.Patil Vidyapeeth, Pune, India approved the protocol for the present study (Ref no. DYPV/EC/101/18). Healthy pre-molar tooth extracted from 5 patients (aged 18–21 years) for orthodontic purposes was used as the source for the DPMSC after obtaining the informed consent. The crown of the extracted tooth was drilled under aseptic conditions to expose its pulp cavity. Broach was used for extirpating the pulp, which was then transported to the laboratory in Dulbecco's modified Eagle's medium (DMEM). The phosphate-buffered saline (PBS) was used to wash the pulp thrice in the sterile cell culture hood. Isolation and characterization of DPSCs were carried out using the explant culture method described previously in (Patil et al., 2018). Briefly, Pulp tissue was minced into tiny fragments, and the pieces were placed in 35 mm polystyrene plastic culture dishes. A sufficient amount of fetal bovine serum (FBS) (Gibco, Rockville, MD, USA) was added to the tissues to cover them completely. Explant tissue containing FBS was incubated at 37 °C and 5% Co2 for 24 h; DPSCs culture system was maintained in DMEM (Invitrogen, Carlsbad, CA, USA) supplemented with 20% FBS and antibiotic–antimycotic solution at similar conditions. The culture medium was replenished twice weekly, and cell growth, health, and morphology were monitored regularly with an inverted phase-contrast microscope. At 70–80% confluence, cells were detached using 0.25% Trypsin-EDTA solution (Invitrogen, Carlsbad, CA, USA) and transferred to a bigger 25-cm^2 polystyrene culture flask (Nunc, Rochester, NY, USA). Subsequently, the cells were subject to continuous passage in the 1:2 ratio for further experiments. Cells from passage 3 to 5 were used in the experimentation.

Once the DPMSC were in the logarithmic phase, they were trypsinized, collected, and subjected to PBS washing (twice). To the above sample, a 500 μL fixative solution was added. Cell concentration was adjusted to $1x10^7$ cells/ml. A fresh Eppendorf tube was used to transfer 100 μL of the suspension. Normal goat serum (50 μL, for 15–20 min at room temperature) was used to block the cells. The sample was incubated for 30 min in the dark with fluorophore tagged anti-CD90-PE, anti-CD73-FITC, anti-CD105-FITC (mesenchymal stem cell markers +), anti-CD34-APC, anti-CD45-APC, (hematopoietic markers –ve), and anti-HLA-DR-PE (MHC class II antigen). The sample was washed with PBS (twice) after incubation to remove the excess antibody. Attune NxT (Thermo Fisher Scientific, Waltham, MA, USA) was used to analyze and quantify the cells. Negative controls used included the FITC, APC, or PE-labeled immunoglobulin G-stained cells (referred to as isotype control).

DPMSC-conditioned medium preparation: For the preparation of DPMSC-conditioned medium (DPMSC-CM), DPMSCs were seeded into T-75 flasks (75 cm^2 surface area) (Nunc, Rochester, NY, USA) at the seeding density of 1 X 10^5 cells per cm^2 with 15 mL of DMEM (Invitrogen, Carlsbad, CA, USA) + 10% FBS (Gibco, Rockville, MD, USA). After 24 h of incubation, the flasks were observed under the microscope to make sure the cells are adhered to the surface of the flasks. Further, the media was replaced with 15 mL of DMEM + 0.2% FBS. Cellular morphology and metabolic activity were also observed to make sure that there is no adverse effect of serum starvation on DPMSCs (results not shown). After 48 h of incubation, the spent medium (DPSC-CM) was aspirated, centrifuged at 300 xg to remove debris, supernatant was taken out in fresh tubes, again filtered by using 0.22-μm syringe filters (Corning, NY, USA) and collected in sterile tubes. The DPMSC-CM was stored at −80 °C until experimental utilization. For experimental use, DPMSC-CM was made-up as DPMSC-CM + 10% FBS. For experimental groups, 20%, 50%, and 100% of this composition was mixed with appropriate amount of complete growth medium (DMEM + 10% FBS). Control groups were incubated with only complete growth medium (DMEM + 10% FBS).

Cancer cell lines: Oral cancer cell line (AW13516), was obtained from the Advanced Centre for Treatment, Research, and Education in Cancer, Tata Memorial Centre, Mumbai, India. Breast cancer cell lines (MDA-MB-231), and melanoma cell lines (A-375) were obtained from National Centre for Cell Science, Pune, India.

Bead-based multiplex assay: LEGENDplex™ Human Growth Factor Panel (13-plex) (Biolegend; Cat. No. 740180) was used to assess angiopoietin-2 (Ang-2), epidermal growth factor (EGF), erythropoietin (EPO), basic fibroblast growth factor (bFGF), granulocyte-colony stimulating factor (G-CSF), granulocyte–macrophage colony-stimulating factor (GM-CSF), hepatocyte growth factor (HGF), macrophage colony-stimulating factor (M−CSF), platelet-derived growth factor-AA (PDGF-AA), PDGF-BB, stem cell factor (SCF), transforming growth factor-alpha (TGF- α), vascular endothelial growth factor (VEGF). For cytokine analysis, LEGENDplex™ Human Essential Immune Response Panel (13-plex) (Biolegend; Cat. No. 740929) was used to assess pro-inflammatory cytokines interleukin 1 beta (IL-1β), tumor necrosis factor-alpha (TNF-α), interleukin 17 A (IL-17A), interleukin 12p70

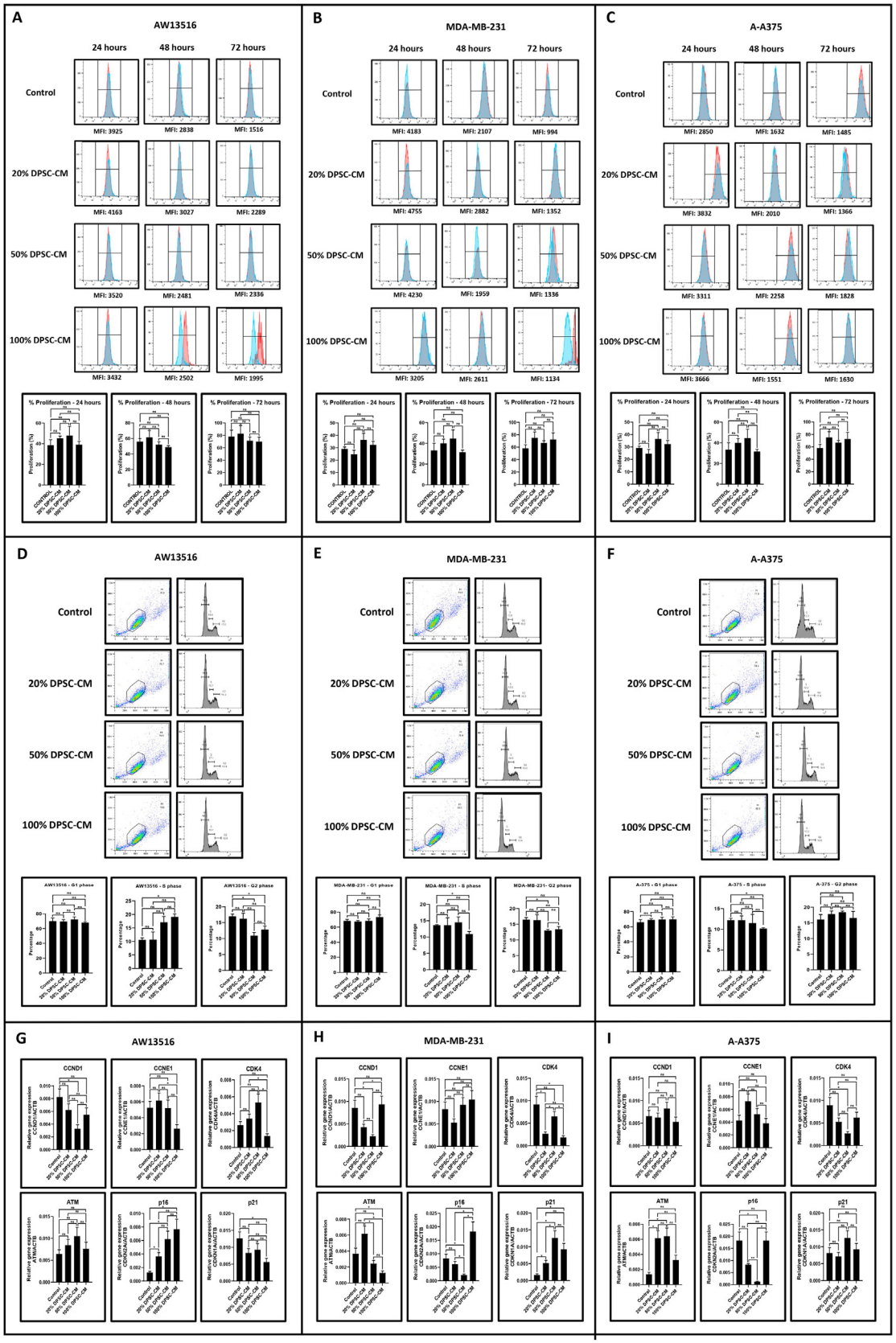
A
AW13516
24 hours
48 hours
72 hours
Control
20% DPSC-CM
50% DPSC-CM
100% DPSC-CM
MFI: 3925
MFI: 2838
MFI: 1516
MFI: 4163
MFI: 3027
MFI: 2289
MFI: 3520
MFI: 2481
MFI: 2336
MFI: 3432
MFI: 2502
MFI: 1995
% Proliferation - 24 hours
% Proliferation - 48 hours
% Proliferation - 72 hours
B
MDA-MB-231
MFI: 4183
MFI: 2107
MFI: 994
MFI: 4755
MFI: 2882
MFI: 1352
MFI: 4230
MFI: 1959
MFI: 1336
MFI: 3205
MFI: 2611
MFI: 1134
C
A-A375
MFI: 2850
MFI: 1632
MFI: 1485
MFI: 3832
MFI: 2010
MFI: 1366
MFI: 3311
MFI: 2258
MFI: 1828
MFI: 3666
MFI: 1551
MFI: 1630
D
AW13516
E
MDA-MB-231
F
A-A375
AW13516 - G1 phase
AW13516 - S phase
AW13516 - G2 phase
MDA-MB-231 - G1 phase
MDA-MB-231 - S phase
MDA-MB-231 - G2 phase
A-375 - G1 phase
A-375 - S phase
A-375 - G2 phase
G
AW13516
H
MDA-MB-231
I
A-A375
CCND1
CCNE1
CDK4
ATM
p16
p21

(IL-12p70), interferon-gamma (IFN-γ), C-X-C motif chemokine ligand 10 (CXCL10), C-C Motif Chemokine Ligand 2 (CCL2), C-C motif chemokine ligand 8 (CXCL8), and anti-inflammatory cytokines interleukin 2 (IL-2), interleukin 4 (IL-4), interleukin 6 (IL-6), interleukin 10 (IL-10), transforming growth factor-beta 1 (TGF-β1). Standard protocols were used according to the manufacturer's instructions. Briefly, 25 μL of the CM from DPMSC-CM was incubated with the microbeads for 2 h. After incubation, the detection antibodies were introduced and incubated for 30 min. Further, the samples were washed with wash buffer and centrifuged at 2000 rpm for 5 min. The supernatant was removed and the pellet was resuspended in 200 μL sheath fluid. The samples were then acquired on a flow cytometer (Attune NxT, Thermo Fisher Scientific, Waltham, MA, USA) and analysis performed using LEGENDplex™ Data Analysis Software (BioLegend, San Diego, CA, USA). The same procedure was used to analyze the CM of cancer cells pre and post-exposure to DPMSC-CM.

RT-PCR: The GeneJet purification columns (Invitrogen, Thermo Scientific, Lithuania) method was employed to extract total RNA from the pelleted cells. Adhering to the manufacturer's instruction of the cDNA synthesis kit, 1 μg RNA was reversely transcribed. SYBR Green PCR master mix (Applied Biosystems, Austin, TX, USA) was employed for quantitative analysis of genes on the QuantStudio 5 Real-Time PCR system (Applied Biosystems, Foster City, CA, USA). Using the ΔΔCt method, the target gene expressions were normalized to GAPDH. By referring to the mean cycle threshold (CT), each gene's CT values were corrected. $2^{-\Delta\Delta Ct}$ method was used to quantify RT-PCR data and to provide a relative gene expression normalized to the average CT for the GAPDH gene. Primers employed for the assessment of various gene expressions are summarized in the supplementary files.

Cell Trace carboxyfluorescein succinimidyl ester (CFSE) assay: CFSE fluorescence cell proliferation kit (Invitrogen, Waltham, MA, USA) was used to assess cell proliferation in cancer cell lines. For obtaining a final working solution, Cell Trace stock solution (1 μL) in DMSO was added to cell suspension in phosphate-buffered saline (PBS). Cells were protected from light and maintained at 37 °C for 20 min. A large amount (6 times the initial volume) of culture medium was added to the cells and was subjected to 5-minute incubations to halt the reaction. In the freshly prepared pre-warmed complete culture medium, the centrifuged cell–cell pellet was resuspended. For the Cell Trace reagent to undergo acetate hydrolysis, the cells were subjected to incubation for at least 10 min. Following incubation, cells were seeded with different media compositions in culture dishes, following which flow cytometry analysis was carried out.

Annexin V/propidium iodide (PI): The supernatant was removed from the harvested cells washed in PBS, then suspended in 1 mL FACS buffer + 2% FBS solution and stained with annexin V-FITC (cell apoptosis marker). Per manufactures instruction (BioLegend), propidium iodide (PI) was added, and subsequently, flow cytometric analysis of cells was carried out on the Attune NxT flow cytometer

Cell cycle analysis: In a 12 well plate, cancer cells were placed for a 24-hour incubation with 5×10^4 cells per well. Cells were treated DPSC conditioned media for 48 h and subjected to PBS washing, 70% ethanol fixation for 2 h at 20 °C. The fixed cells were subjected to RNase treatment (10 mg/ml) and PI (Sigma-Aldrich Corp., St. Louis, MO, USA) staining at room temperature for 30 min in the dark. Flow cytometry was used to measure the individual nuclei PI fluorescence, based on which the cell percentages in various cell cycle phases were estimated.

DNA fragmentation assay: The cancer cells were prepared as instructed in the cytotoxicity assay technique and further used for estimation of DNA fragmentation index in the control and experimental groups. Enzyme-linked immunosorbent assay (ELISA) was performed by using Cell Death Detection ELISA PLUS (Roche, Indianapolis, IN, USA) for quantitative measurement of cytoplasmic Histone-associated DNA fragments as a degree of cell death. The absorbance values taken at 405 nm were normalized to percentage.

3. Results

DPMSC-CM induces AW13516 apoptosis, inhibits proliferation, migration, stemness, but augments potential for invasiveness, adhesion, multi-drug resistance, DNA repair, and mitochondrial repair: DPMSC-CM inhibited the proliferation of AW13516 (Fig. 1a). The inhibition could have been mediated through the augmented p16 expression (Fig. 1g), which in turn could have caused cyclin D1 downregulation (Fig. 1g). Despite cyclin D1 attenuation, it failed to arrest the cell cycle at the G1 phase (Fig. 1d). Instead, the cell cycle arrest was noted in the cyclin E regulated S phase, albeit cyclin E expression in itself not significantly altered (Fig. 1d). DPMSC-CM induced apoptosis on cancer cells with concurrent caspase 9 upregulation mediated through the intrinsic pathway (Fig. 2a, d, g). On the contrary, p21 was attenuated which could have aided in cell cycle progression at the G2 phase, instead paradoxically failed to inhibit proliferation nor increase apoptosis of cancer cells as might be expected (Fig. 2a, d, g). Cancer stemness, EMT, and migration-related gene expressions were attenuated (Fig. 3a, d, g, 4a). The genes related to invasion, adhesion, multi-drug resistance, DNA repair, and mitochondrial repair were significantly upregulated (Fig. 3d, g, j, 4d, g). The pro-carcinogenic effects (increased invasion, adhesion, multi-drug resistance, DNA repair, and mitochondrial repair) of DPMSC-CM could be largely attributed to the upregulation of growth factors Ang-2, EGF, M−CSF, PDGF-AA, PDGF-BB, and pro-inflammatory cytokines TNF-α, IL-2, downregulation of anti-inflammatory cytokine TGF-β1, and pro-inflammatory cytokine IL-4 (Fig. 5a, d). DPMSC-CM anti-carcinogenic effect (decreased proliferation, increased apoptosis, decreased stemness, migration, and EMT) could be largely attributed to attenuated levels of growth factors EPO, EGF, pro-inflammatory cytokine CXCL-10, and anti-inflammatory cytokine IL-10 (Fig. 5a, d).

DPMSC-CM induces MDA-MB-231 apoptosis, inhibits proliferation, migration, and adhesion, but augments invasion, and multi-drug resistance: DPMSC-CM inhibited the proliferation of MDA-MB-231 (Fig. 1b). This is likely secondary to the upregulation

Fig. 1. DPMSC-S inhibited the proliferation of AW13516, MDA-MB-231, and A375 cell lines by modulating the cell cycle regulators. AW13516, MDA-MB-231, and A375 cell lines were treated with 20%, 50%, and 100% DPMSC-CM for 24, 48, and 72 h and proliferation of cancer cells was assessed by CFSE assay. (a) Comparative analysis of proliferation in AW13516 cell line. (b) Com-parative analysis of proliferation in MDA-MB-231 cell line. (c) Comparative analysis of proliferation in A375 cell line. AW13516, MDA-MB-231, and A375 cell lines were treated with 20%, 50%, and 100% DPMSC-CM for 48 h, and cell cycle phases i.e. G1, S, and G2 in cancer cells were assessed by flow cytometry and gene expression analysis for cell cycle-related genes CCND1, CCNE1, CDK4, ATM, CDKN2A, and CDKN1A was per-formed by RT-qPCR. (d) Comparative analysis of cell cycle phase distribution in AW13516 cell line. (e) Comparative analysis of cell cycle phase distribution in MDA-MB-231 cell line. (f) Comparative analysis of cell cycle phase distribution in A375 cell line. (g) Comparative analysis of expression of genes regulating cell cycle phases in AW13516 cell line. (h) Comparative analysis of expression of genes regulating cell cycle phases in the MDA-MB-231 cell line. (i) Comparative analysis of expression of genes regulating cell cycle phases in A375 cell line. Experiments were performed in triplicates and repeated 2 times. ns not significant, $^*p < 0.05$, $^{**}p < 0.01$.

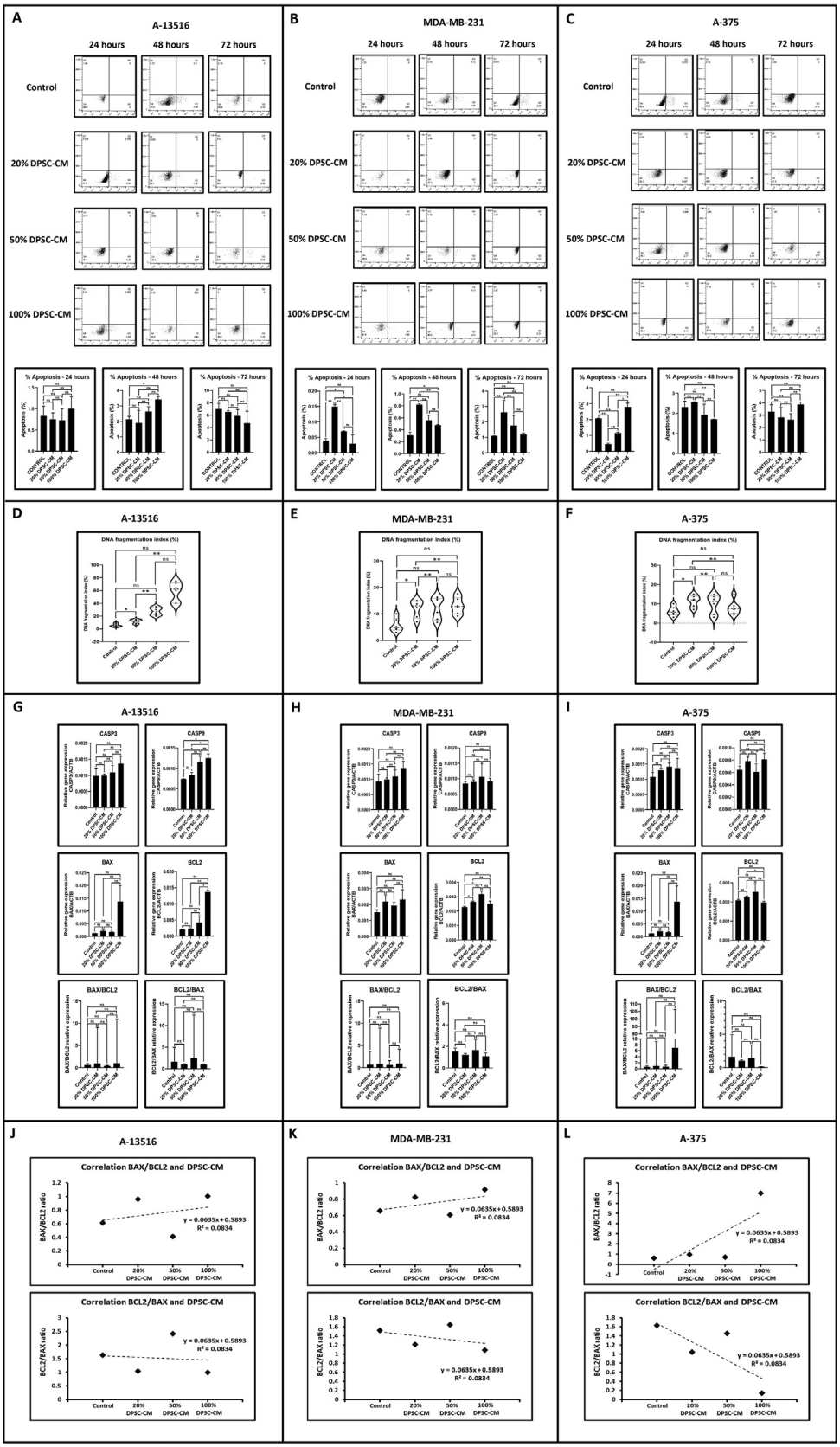
A
A-13516
24 hours
48 hours
72 hours
Control
20% DPSC-CM
50% DPSC-CM
100% DPSC-CM
% Apoptosis - 24 hours
% Apoptosis - 48 hours
% Apoptosis - 72 hours
B
MDA-MB-231
C
A-375
D
A-13516
DNA fragmentation index (%)
E
MDA-MB-231
F
A-375
G
A-13516
CASP3
CASP9
BAX
BCL2
BAX/BCL2
BCL2/BAX
H
MDA-MB-231
I
A-375
J
A-13516
Correlation BAX/BCL2 and DPSC-CM
BAX/BCL2 ratio
y = 0.0635x + 0.5893
R² = 0.0834
Correlation BCL2/BAX and DPSC-CM
BCL2/BAX ratio
K
MDA-MB-231
L
A-375

of p21 which in turn downregulates cyclin D1 and CDK4 (Fig. 1h). DPMSC-CM induced apoptosis on cancer cells (Fig. 2b). ATM and p16 expression were attenuated, which could have allowed cell cycle progression in the S and G2 phase, albeit without any significant inhibition of proliferation nor augmentation of apoptosis on the cancer cells (Fig. 1b, e, h, 2b, e, h). Cancer migration and adhesion were attenuated (Fig. 3e, h, k). The genes related to invasion and multi-drug resistance were significantly upregulated (Fig. 4e, h). DPMSC-CM pro-carcinogenic effects (increased invasion, and multi-drug resistance) in our experiments are largely attributed to augmented growth factors EGF, EPO, G-CSF, HGF, M−CSF, PDGF-AA, and pro-inflammatory cytokine TNF-α, CXCL10, IL-12p70. DPMSC-CM anti-carcinogenic effect (decreased proliferation, increased apoptosis, decreased migration, and adhesion) were likely secondary to attenuated levels of growth factors EPO, pro-inflammatory cytokines CCL2, CXCL10, CXCL8, and augmented levels of anti-inflammatory cytokines IL-2 (Fig. 5b, e).

DPMSC-CM induces A-375 apoptosis, inhibits proliferation, but augments invasion, migration, adhesion, stemness, and EMT: DPMSC-CM inhibited the proliferation of A-375 by augmenting ATM which in turn downregulated CDK4 (Fig. 1c, i). DPMSC-CM induced apoptosis on the cancer cells (Fig. 2c, f). p16 was attenuated, resulting in cell cycle progression at the S phase, despite not inhibiting proliferation nor augmenting apoptosis (Fig. 1c, f, i, 2c, f). Stemness showed differential effect (augmented OCT-4 and attenuated SOX-2), while the genes related to EMT, invasion, migration, adhesion were significantly upregulated (Fig. 3c, f, i, l, 4c, f). DPMSC-CM pro-carcinogenic effects (increased EMT, invasion, migration, and adhesion) can be largely attributed to upregulation of growth factors Ang-2, EGF, PDGF-BB, TGF-α, pro-inflammatory cytokines TNF-α, and IL-17A (Fig. 5c, f). DPMSC-CM anti-carcinogenic effect (decreased proliferation) can be largely attributed to attenuated levels of growth factors EGF, EPO, FGF-basic, PDGF-AA, PDGF-BB, pro-inflammatory cytokine CXCL8, augmented levels of growth factor SCF, anti-inflammatory cytokine IL-2, and pro-inflammatory cytokine CXCL10 (Fig. 5c, f).

DPMSC-CM has shown dual effects in our experiments by exhibiting both pro-tumorigenic and anti-tumorigenic properties at varying levels. While it has the potential to inhibit cancer cell proliferation, it paradoxically augmented key carcinogenic properties including invasion in all 3 cancer lines.

4. Discussion

The global cancer incidence is on a steady rise at 19.3 million with resultant 10 million deaths annually as of 2020 (Sung et al., 2021), this translates into a tremendous economic impact sprawling around US$161.2 and €57.3 billion in the United States and European Union alone (“The Economic Burden of Cancer | The Cancer Atlas, xxxx” n.d.).

There is a massive outpouring of resources to help mitigate this ongoing modern-day health care crisis on basic science, translational and clinical research fronts with support from government to major institutions and the highly incentivized pharmaceutical industry. This has helped several groundbreaking innovations into the molecular understanding of cancer and its therapy. Breast cancer ranks 1st among women with an annual incidence of 2.3 million (11.7%), there have been significant advances in treatment leading to long overall and disease-free survival rates compared to other cancers (Sung et al., 2021). Melanoma survival rates vary widely based on the stage with > 90% to < 30% 5-year survival for localized and distant disease (Costa Svedman et al., 2016). Oral cancer has a 5-year overall survival rate of 64.4% and a disease-specific survival rate of 79.3% (Zanoni et al., 2019).

The premise of our study is based on the multi-modal targeted approach in cancer management and its subsequent advances. These include surgery, chemotherapy, and radiotherapy ultimately requiring some form of reconstruction based on the specific cancer sub-type, anatomical location, and treatment-related morbidity.

Cancer patient’s post-treatment rehabilitation includes tissue regeneration and/ or amelioration of radiation-induced fibrosis. Mesenchymal stem cells and their secretome as detailed in our introduction has had a major surge in industry-wide cancer-related regeneration and reconstructive applications. While this is encouraging, it is imperative to understand that all cancers declared to have R0 resection (Microscopically margin-negative resection) can still harbor islands of micrometastasis and in-transit lesions, presence of synchronous and metachronous lesions, or in the case of breast cancer, multi-centric or multi-focal lesions that could be missed while targeting the primary lesion. These factor towards metastasis in oral cancer (Warshavsky et al., 2019), breast cancer (Pérez-González et al., 2017; Wang et al., 2020), and melanoma (Rajaee et al., 2021), and recurrence associated with cancers of the oral cavity (Lenze et al., 2020), breast (Wang et al., 2020), and melanoma (Costa Svedman et al., 2016). In light of this, our study questioned the safety profile using mesenchymal stem cells and their secretome for reconstruction and tissue regeneration post-cancer treatment as discussed. Based on a systematic review of the literature published in 2021 by our research team (Raj et al., 2021), it is apparent that MSC-derived conditioned media have shown potential for pro-carcinogenic effect against specific cancer cell lines, including DPMSC-CM pro-carcinogenic effect on the prostate cancer lines (Doğan et al., 2017). Thus, introducing them to cancer patients could increase the risk of disease progression which could potentially be mediated through augmentation of one or more carcinogenic properties

To assess if DPMSC pro-carcinogenic potential extended on to other cancer types especially those which could be encountered by DPMSC-CM clinical application in oral rehabilitation, wound healing, and anti-fibrotic effect. The results elicit a differential effect on the cancer cell lines which was both time and dose-dependent. The differential effect in the present study represents

Fig. 2. DPMSC-S induced apoptosis in AW13516, MDA-MB-231, and A375 cell lines. AW13516, MDA-MB-231, and A375 cell lines were treated with 20%, 50%, and 100% DPMSC-CM for 24, 48, and 72 h and apoptosis of cancer cells was assessed by Annexin V assay. (a) Comparative analysis of apoptosis in AW13516 cell line. (b) Comparative analysis of apoptosis in MDA-MB-231 cell line. (c) Comparative analysis of apoptosis in A375 cell line. AW13516, MDA-MB-231, and A375 cell lines were treated with 20%, 50%, and 100% DPMSC-CM for 48 h, and DNA fragmentation index in cancer cells was assessed by spectrophotometry. (d) Comparative analysis of DNA fragmentation index in AW13516 cell line. (e) Comparative analysis of DNA fragmentation index in the MDA-MB-231 cell line. (f) Comparative analysis of DNA fragmentation index in A375 cell line. AW13516, MDA-MB-231, and A375 cell lines were treated with 20%, 50%, and 100% DPMSC-CM for 48 h, and gene expression analysis for apoptosis-related genes CASP3, CASP9, BAX, BCL2, BAX/BCL2 ratio, and BCL2/BAX ratio was performed by RT-qPCR. (g) Comparative analysis of expression of apoptotic genes in AW13516 cell line. (h) Comparative analysis of expression of apoptotic genes in the MDA-MB-231 cell line. (i) Comparative analysis of expression of apoptotic genes in A375 cell line. BAX/BCL2 and BCL2/BAX ratios were calculated and correlated with the DPMSC-CM concentrations. (j) Correlation between BAX/BCL2 and DPMSC-CM and BCL2/BAX and DPMSC-CM in AW13516 cell line. (k) Correlation between BAX/BCL2 and DPMSC-CM and BCL2/BAX and DPMSC-CM in MDA-MB-231 cell line. (j) Correlation between BAX/BCL2 and DPMSC-CM and BCL2/BAX and DPMSC-CM in A375 cell line. Experiments were performed in triplicates and repeated 2 times. ns not significant, $^{*}p < 0.05$, $^{**}p < 0.01$.

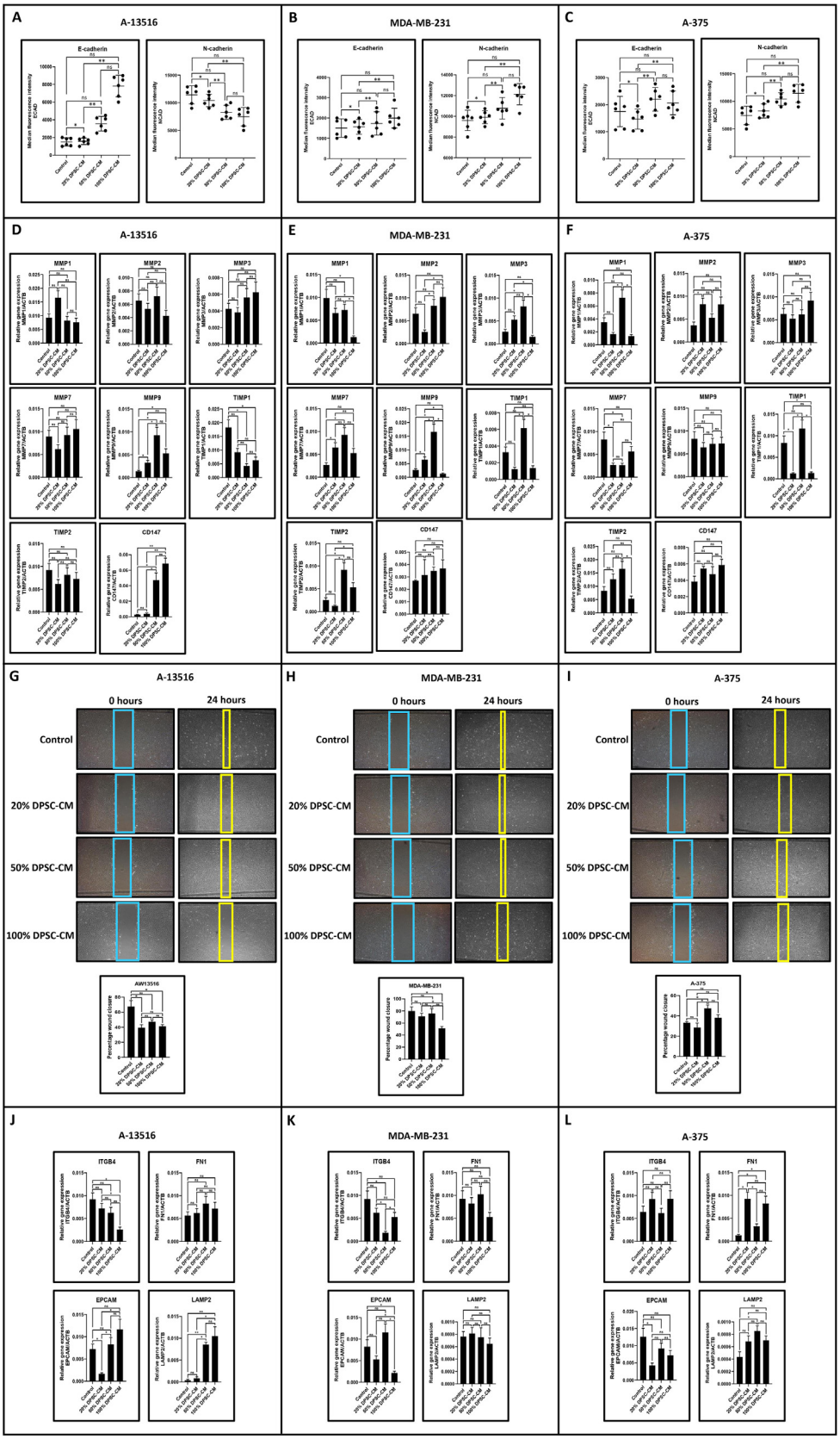
A
A-13516
E-cadherin
N-cadherin
B
MDA-MB-231
E-cadherin
N-cadherin
C
A-375
E-cadherin
N-cadherin
D
A-13516
MMP1
MMP2
MMP3
MMP7
MMP9
TIMP1
TIMP2
CD147
E
MDA-MB-231
MMP1
MMP2
MMP3
MMP7
MMP9
TIMP1
TIMP2
CD147
F
A-375
MMP1
MMP2
MMP3
MMP7
MMP9
TIMP1
TIMP2
CD147
G
A-13516
0 hours
24 hours
Control
20% DPSC-CM
50% DPSC-CM
100% DPSC-CM
AW13516
Percentage wound closure
H
MDA-MB-231
0 hours
24 hours
Control
20% DPSC-CM
50% DPSC-CM
100% DPSC-CM
MDA-MB-231
Percentage wound closure
I
A-375
0 hours
24 hours
Control
20% DPSC-CM
50% DPSC-CM
100% DPSC-CM
A-375
Percentage wound closure
J
A-13516
ITGB4
FN1
EPCAM
LAMP2
K
MDA-MB-231
ITGB4
FN1
EPCAM
LAMP2
L
A-375
ITGB4
FN1
EPCAM
LAMP2

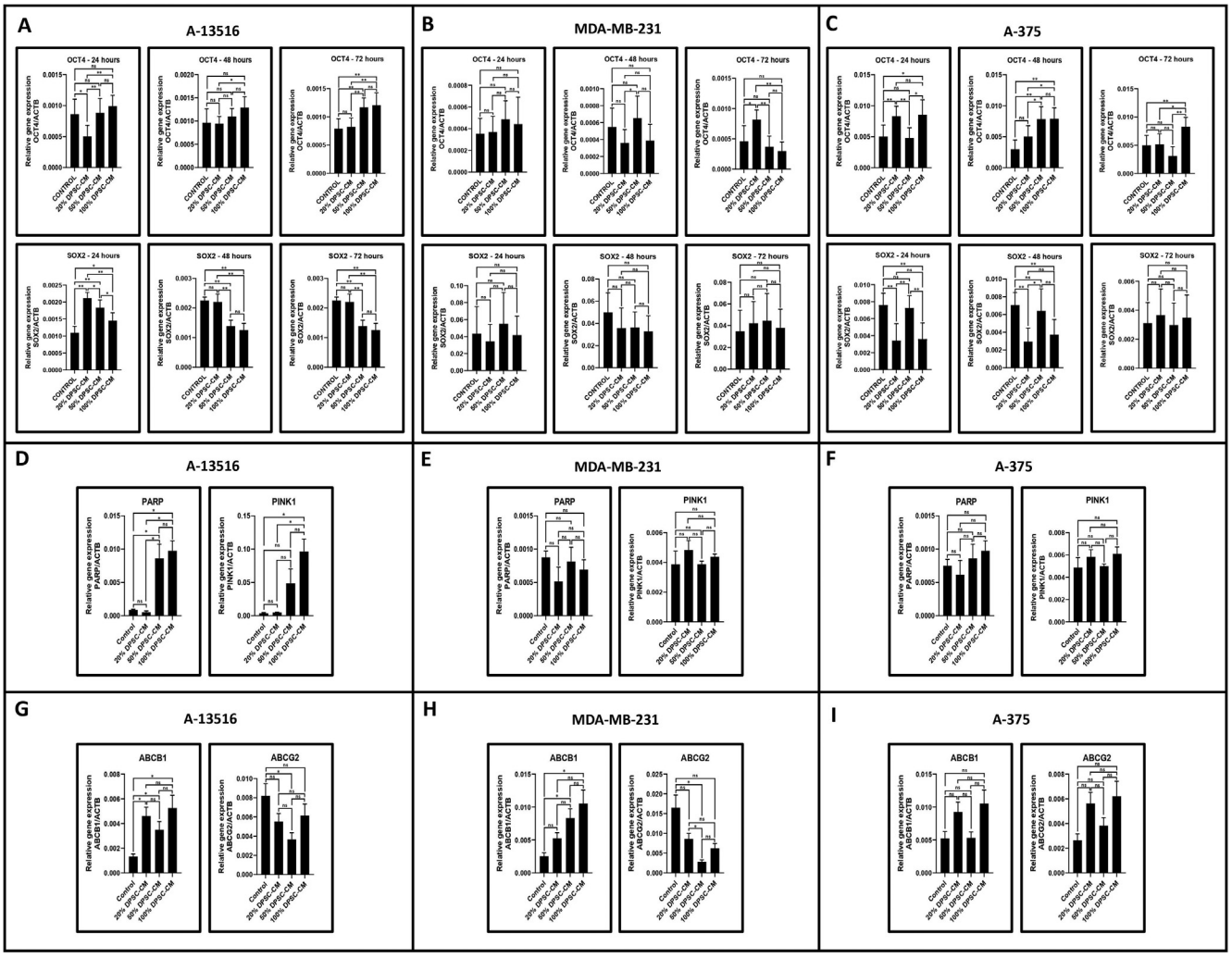

Fig. 4. DPMSC-S upregulated genes related to multi-drug resistance, DNA repair, and mitochondrial repair in AW-13516; multi-drug resistance in MDA-MB-231, while downregulating gene related to stemness in AW13516. AW13516, MDA-MB-231, and A375 cell lines were treated with 20%, 50%, and 100% DPMSC-CM for 24, 48, and 72 h and gene expression analysis for stemness related genes OCT4 and SOX2 was performed by RT-qPCR. (a) Comparative analysis of expression of stemness-related genes in AW13516 cell line. (b) Comparative analysis of expression of stemness-related genes in the MDA-MB-231 cell line. (c) Comparative analysis of expression of stemness-related genes in A375 cell line. AW13516, MDA-MB-231, and A375 cell lines were treated with 20%, 50%, and 100% DPMSC-CM for 48 h, and gene expression analysis for DNA repair genes PARP and PINK1 was performed by RT-qPCR. (d) Comparative analysis of expression of DNA repair genes in AW13516 cell line. (e) Comparative analysis of expression of DNA repair genes in the MDA-MB-231 cell line. (f) Comparative analysis of expression of DNA repair genes in A375 cell line. AW13516, MDA-MB-231, and A375 cell lines were treated with 20%, 50%, and 100% DPMSC-CM for 48 h, and gene expression analysis for multidrug resistance genes ABCB1 and ABCG2 were performed by RT-qPCR. (g) Comparative analysis of expression of multidrug resistance genes in AW13516 cell line. (h) Comparative analysis of expression of multidrug resistance genes in the MDA-MB-231 cell line. (i) Comparative analysis of expression of multidrug resistance genes in A375 cell line. Experiments were performed in triplicates and repeated 2 times. ns not significant, $^{*}p < 0.05$, $^{**}p < 0.01$.

Fig. 3. DPMSC-S upregulated genes related to invasion, and adhesion in AW-13516; invasion in MDA-MB-231; EMT, invasion, migration, and adhesion in A-375, while downregulating gene related to migration, and EMT in AW13516; migration, and adhesion in MDA-MB-231. AW13516, MDA-MB-231, and A375 cell lines were treated with 20%, 50%, and 100% DPMSC-CM for 48 h, and EMT markers E-cadherin and N-cadherin in cancer cells was assessed by flow cytometry. (a) Comparative analysis of EMT markers in AW13516 cell line. (b) Comparative analysis of EMT markers in the MDA-MB-231 cell line. (c) Comparative analysis of EMT markers in A375 cell line. AW13516, MDA-MB-231, and A375 cell lines were treated with 20%, 50%, and 100% DPMSC-CM for 48 h and gene expression analysis for invasion related genes MMP1, MMP2, MMP3, MMP7, and MMP9 and metastasis-related genes TIMP1, TIMP2, and CD147 were performed by RT-qPCR. (d) Comparative analysis of expression of invasion and metastasis-related genes in AW13516 cell line. (e) Comparative analysis of expression of invasion and metastasis-related genes in the MDA-MB-231 cell line. (f) Comparative analysis of expression of invasion and metastasis-related genes in A375 cell line. Wound healing scratch assay was performed to assess migration of AW13516, MDA-MB-231, and A375 cell lines treated with 20%, 50%, and 100% DPMSC-CM for 24 h and gene expression analysis for adhesion-related genes ITGB4, FN1, and EPCAM and migration-related gene LAMP2 was performed by RT-qPCR. (g) Comparative analysis of migration in AW13516 cell line. (h) Comparative analysis of migration in MDA-MB-231 cell line. (i) Comparative analysis of migration in A375 cell line. (j) Comparative analysis of expression of adhesion and migration-related genes in AW13516 cell line. (k) Comparative analysis of expression of adhesion and migration-related genes in the MDA-MB-231 cell line. (l) Comparative analysis of expression of adhesion and migration-related genes in A375 cell line. Experiments were performed in triplicates and repeated 2 times. ns not significant, $^{*}p < 0.05$, $^{**}p < 0.01$.

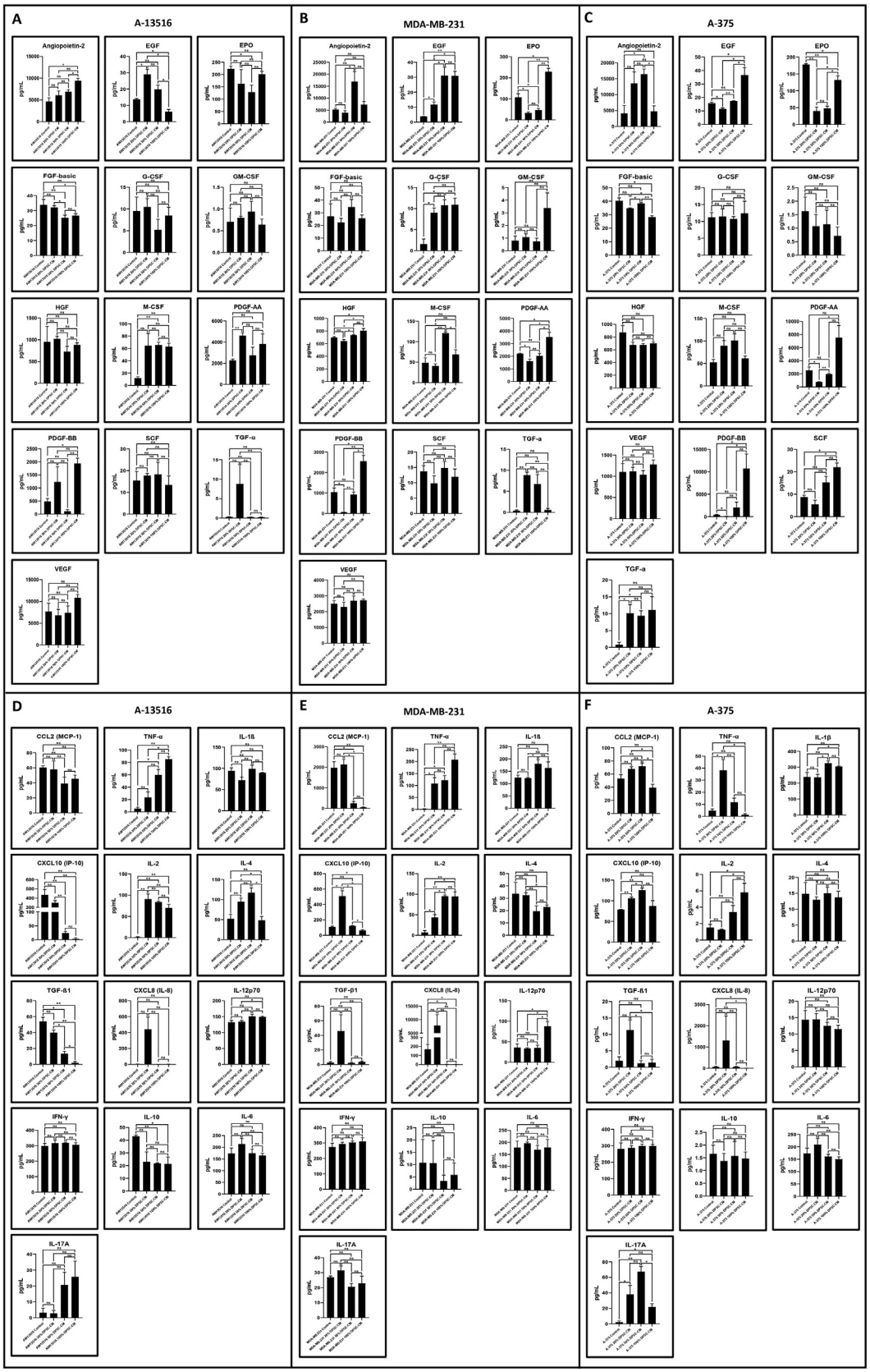
A
A-13516
Angiopoietin-2
EGF
EPO
FGF-basic
G-CSF
GM-CSF
HGF
M-CSF
PDGF-AA
PDGF-BB
SCF
TGF-α
VEGF
B
MDA-MB-231
Angiopoietin-2
EGF
EPO
FGF-basic
G-CSF
GM-CSF
HGF
M-CSF
PDGF-AA
PDGF-BB
SCF
TGF-a
VEGF
C
A-375
Angiopoietin-2
EGF
EPO
FGF-basic
G-CSF
GM-CSF
HGF
M-CSF
PDGF-AA
VEGF
PDGF-BB
SCF
TGF-a
D
A-13516
CCL2 (MCP-1)
TNF-α
IL-1ß
CXCL10 (IP-10)
IL-2
IL-4
TGF-ß1
CXCL8 (IL-8)
IL-12p70
IFN-γ
IL-10
IL-6
IL-17A
E
MDA-MB-231
CCL2 (MCP-1)
TNF-α
IL-1ß
CXCL10 (IP-10)
IL-2
IL-4
TGF-ß1
CXCL8 (IL-8)
IL-12p70
IFN-γ
IL-10
IL-6
IL-17A
F
A-375
CCL2 (MCP-1)
TNF-α
IL-1β
CXCL10 (IP-10)
IL-2
IL-4
TGF-ß1
CXCL8 (IL-8)
IL-12p70
IFN-γ
IL-10
IL-6
IL-17A

the varying degree of inhibition or augmentation of one or more carcinogenic properties of each cell line. Although DPMSC-CM did show significant anti-carcinogenic effects on all the 3 cancer cell lines including inhibition of cell proliferation, augmentation of apoptosis, there were significant pro-carcinogenic effects - potential for invasion, migration, stemness, multidrug resistance, and adhesion. Our primary objective was to assess pro-carcinogenic effects mediated by DPMSC-CM and hence will focus primarily on it in our discussion.

DPMSC-CM induced pro-carcinogenic effects noted in the present study are in par with Dogan et al who observed that DPMS-CM increased cell viability, inhibited apoptosis in the PC-3 (prostate cancer cell line), by increasing the expression of anti-apoptotic marker (Bcl-2) and decreasing the expression of pro-apoptotic marker (BAX). DPMSC-CM also caused upregulation of Col 1, fibronectin, and laminin 2 in PC-3 indicating an enhanced migratory potential. Dogan et al attributed the pro-carcinogenic effect of DPMSC-CM to its growth factors, although the secretome profile was not delineated to identify the involved secretory factors. Rizvanov et al [10] in 2010 co-cultured human third molar tooth germ stem cells (TGMSCs) with SH-SY5Y cells (neuroblastoma cell lines). The cancer cells were subjected to hydrogen peroxide-induced stress. They observed that despite the toxicity of the hydrogen peroxide, TGMSCs significantly increased the viability of SH-SY5Y cells. Based on the results they suggested TGSCs possess a neuroprotective effect, which in turn was largely attributed to the secretome of the stem cells, which again was not profiled in the study. In 2011, Yalvac et al demonstrated that MSC-CM from TGSCs significantly reduced doxorubicin/hydrogen peroxide-induced neurotoxicity and increased cell viability in SH-SY5Y [11]. Yalvac et al study provided further evidence that the secretome/CM derived from the stem cell could be the primary effector of the changes induced in the cancer cell. Based on the results from their co-culture study [11] and Rizvanov et al [10] assessment, Yalvac et al in 2013 [12] assessed various growth factors and cytokines present in the TGSC-CM. ELISA-based cytokines, chemokines, and growth factors analysis revealed the presence of TGF-b1, IL-8, VEGF, IL-5, IL-6, FGF2, BMP-2, and IL-10. These factors were suggested to be the primary effectors for the pro-carcinogenic effects noted in the cancer cell lines.

Based on the understanding of the critical role of the DPMSC CM, the present study initially profiled DPMSC-CM and identified levels of growth factors, pro-and anti-inflammatory cytokines. Also, the cancer cell line secretome was profiled before and after exposure to the DPMSC-CM. The cancer cell secretome post-DPMSC-CM exposure showed significant changes in the levels of growth factors, pro-inflammatory cytokines, and anti-inflammatory cytokines. These cancer cell secretome changes correlated with changes imparted in various carcinogenic properties of the cancer cells.

The significantly augmented growth factors implicated in the progression of AW13516 in the present study were Ang-2, EGF, M−CSF, PDGF-AA, PDGF-BB. In oral cancer, Ang-2 has been shown to have an inverse association with a patient's survival and is implicated in augmenting the angiogenesis and vessel maturation of the cancerous tissue, and is significantly correlated with a positive nodal stage (Chien et al., 2008; Li et al., 2013). An augmented EGF level is also closely associated with a positive nodal metastasis, advanced stage, culminating in overall poor survival in oral cancer (Lin et al., 2018). An augmented M−CSF is associated with increased infiltration of tumor-associated macrophages and reduces survival rate in oral cancer (Guo et al., 2020). PDGA-AA has shown to be a VEGF regulator augmenting angiogenesis in oral cancer tissue, potentiating metastasis (Obayashi-Ishii et al., 2018). PDGA-BB has also been shown to have a strong correlation with nodal metastasis and poor survival outcome in oral cancer (Lin et al., 2020).

The significantly augmented growth factors implicated in the progression of MDA-MB-231 in the present study were EGF, EPO, G-CSF, HGF, M−CSF, and PDGF-AA. EGF has been shown to augment the migratory potential of breast cancer cells (González-González et al., 2019). EPO augments microvessel formation and attenuates apoptosis, aiding in breast cancer progression (Jin et al., 2015). G-CSF is associated with a poor overall survival rate in breast cancer (Hollmén et al., 2016). HGF has shown the ability to augment the invasive potential of breast cancer cells (Kuang et al., 2017). M−CSF was shown to be closely associated with metastasis and disease-specific mortality in breast cancer (Richardsen et al., 2015). PDGA-AA is associated with promoting breast cancer cell growth (Yu et al., 2015).

The significantly augmented growth factors implicated in the progression of A-375 in the present study were Ang-2, EGF, PDGF-BB, TGF-α. Ang-2 has been shown to augment metastatic potential in melanoma (Abdul Pari et al., 2020). Augmented EGF levels have been shown to increase the risk of metastasis in melanoma (Bracher et al., 2013). PDGA-BB is shown to augment the proliferation of melanoma cell lines by enhancing its vascular supply (BARNHILL et al., 1996). TGF-α has been shown to aid in the progression of melanoma cells (Krasagakis et al., 1995).

The significantly augmented pro-inflammatory cytokines implicated in the progression of AW-13516 are TNF-α and IL-2. TNF-α has been reported to augment the proliferation of the oral cancer cells aiding in disease progression (Qiu et al., 2018). The significantly attenuated anti-inflammatory cytokine implicated in the progression of AW-13516 is TGF-β1. Increased TGF-β1 is associated with increased overall survival in oral cancer (Elahi and Rakhshan, 2020), thus a reduced TGF- β1 as seen in the present study could have augmented one or more of the carcinogenic properties.

The significantly augmented pro-inflammatory cytokines implicated in the progression of MDA-MB-231 are TNF-α, CXCL10, and IL-12p70. TNF-α was associated with an increased risk of metastasis in breast cancer cells (Ma et al., 2017). CXCL10 has been shown to augment proliferation and chemoresistance in breast cancer cells (Wu et al., 2020). IL-12 has also been closely associated with breast cancer progression (Hussein et al., 2004).

The significantly augmented pro-inflammatory cytokines implicated in the progression of A-375 are TNF-α and IL-17A. TNF-α has been shown to augment the invasive potential of melanoma cells

Fig. 5. DPMSC-S induced significant alterations in the growth factor, pro-inflammatory and anti-inflammatory cytokine levels of AW13516, MDA-MB-231, and A375 cell lines: AW13516, MDA-MB-231, and A375 cell lines were treated with 20%, 50%, and 100% DPMSC-CM for 48 h, and conditioned media from these cells were collected post 48 h of treatment to perform flow cytometry-based growth factor analysis in the secretome for Angiopoietin-2, EGF, EPO, FGF basic, G-CSF, GM-CSF, HGF, M−CSF, PDGF-AA, PDGF-BB, SCF, TGF-α, VEGF. (a) Comparative analysis of growth factors in AW13516 cell line secretome. (b) Comparative analysis of growth factors in MDA-MB-231 cell line secretome. (c) Comparative analysis of growth factors in A375 cell line secretome. AW13516, MDA-MB-231, and A375 cell lines were treated with 20%, 50%, and 100% DPMSC-CM for 48 h, and conditioned media from these cells were collected post 48 h of treatment to perform flow cytometry-based cytokine analysis in the secretome for IL-4, IL-2, CXCL10, IL-1β, TNF-α, CCL2, IL-17A, IL-6, IL-10, IFN-γ, IL-12p70, CXCL8, TGF-β1. (d) Comparative analysis of cytokines in AW13516 cell line secretome. (e) Comparative analysis of cytokines in MDA-MB-231 cell line secretome. (f) Comparative analysis of cytokines in A375 cell line secretome. Experiments were performed in triplicates and repeated 2 times. ns not significant, $^{*}p < 0.05$, $^{**}p < 0.01$.

by upregulating MMP-2 (Rossi et al., 2018). IL-17 has also been shown to aid in the progression of melanoma (Li et al., 2014). The clinical implication of the present study was to emphasize the need for assessing the safety of applying MSCS-S on cancer patients. Before the clinical application of either the MSCs or the MSCs derived products, it is essential to confirm if they do not possess any pro-carcinogenic effect in cancer patients.

5. Conclusions

Our study reflects the dual effects of DPMSC-CM capable of mediating pro and anti-tumorigenesis. The premise of our study is to ensure patient safety by delineating carcinogenic potentiating by mesenchymal stem cell secretome if the microenvironment would harbor tumor cells. The pro-carcinogenic effect of AW13516 could be attributed to augmented levels of Ang-2, EGF, M−CSF, PDGF-AA, PDGF-BB, TNF-α, IL-2, and attenuated level of TGF-β1. The pro-carcinogenic effect of MDA-MB-231 could be attributed to augmented levels of EGF, EPO, G-CSF, HGF, M−CSF, PDGF-AA, TNF-α, CXCL10, and IL-12p70. The pro-carcinogenic effect of A-375 could be attributed to augmented levels of Ang-2, EGF, PDGF-BB, TGF-α, TNF-α, and IL-17A. The limitations of the present study are inherent limitations of clinical applicability stemming from the in-vitro nature of the study devoid of host tumor microenvironment and immunogenicity. Animal model-based molecular delineation would be the next step to validate the in-vitro findings and ensure the long-term durability of the proposed clinical applications with DPMSC-CM. Readers must infer the results of our study accounting for its limitations and the need for further understanding into our findings. We believe it is quintessential to perform animal model studies to ensure safety and devise mechanistic to mitigate any pro-carcinogenic effects by DPMSC-CM before full-fledged human application.

Funding

This research received no external funding.

Institutional Review Board Statement

The study was conducted according to the guidelines of the Declaration of Helsinki, and approved by the Institutional Review Board of Dr.D.Y.Patil Vidyapeeth, Pune, India (Ref no. DYPV/EC/101/18).

Declaration of Competing Interest

The authors declare that they have no known competing financial interests or personal relationships that could have appeared to influence the work reported in this paper.

Appendix A. Supplementary material

Supplementary data to this article can be found online at https://doi.org/10.1016/j.sjbs.2021.07.029.

References

Abdul Pari, A.A., Singhal, M., Hübers, C., Mogler, C., Schieb, B., Gampp, A., Gengenbacher, N., Reynolds, L.E., Terhardt, D., Géraud, C., Utikal, J., Thomas, M., Goerdt, S., Hodivala-Dilke, K.M., Augustin, H.G., Felcht, M., 2020. Tumor caell-derived angiopoietin-2 promotes metastasis in melanoma. Cancer Res. 80, 2586–2598. https://doi.org/10.1158/0008-5472.CAN-19-2660.

Aryan, A., Bayat, M., Bonakdar, S., Taheri, S., Haghparast, N., Bagheri, M., Piryaei, A., Abdollahifar, M.-A., 2018. Human bone marrow mesenchymal stem cell conditioned medium promotes wound healing in deep second-degree burns in male rats. Cells Tissues Organs 206 (6), 317–329. https://doi.org/10.1159/000501651.

Barbier, L., Ramos, E., Mendiola, J., Rodriguez, O., Santamaria, G., Santamaria, J., Arteagoitia, I., 2018. Autologous dental pulp mesenchymal stem cells for inferior third molar post-extraction socket healing: A split-mouth randomised clinical trial. Med. Oral Patol. Oral y Cir. Bucal 0–0. https://doi.org/10.4317/medoral.22466

Barnhill, R.L., Xiao, M., Graves, D., Antoniades, H.N., 1996. Expression of platelet-derived growth factor (PDGF)-A, PDGF-B and the PDGF-alpha receptor, but not the PDGF-beta receptor, in human malignant melanoma in vivo. Br. J. Dermatol. 135, 898–904. https://doi.org/10.1046/j.1365-2133.1996.d01-1092.x.

Bracher, A., Cardona, A.S., Tauber, S., Fink, A.M., Steiner, A., Pehamberger, H., Niederleithner, H., Petzelbauer, P., Gröger, M., Loewe, R., 2013. Epidermal growth factor facilitates melanoma lymph node metastasis by influencing tumor lymphangiogenesis. J. Invest. Dermatol. 133 (1), 230–238. https://doi.org/10.1038/jid.2012.272.

Chen, Z.-Y., Hu, Y.-Y., Hu, X.-F., Cheng, L.-X., 2018. The conditioned medium of human mesenchymal stromal cells reduces irradiation-induced damage in cardiac fibroblast cells. J. Radiat. Res. 59, 555–564. https://doi.org/10.1093/jrr/rry048.

Chien, C.-Y., Su, C.-Y., Chuang, H.-C., Fang, F.-M., Huang, H.-Y., Chen, C.-M., Chen, C.-H., Huang, C.-C., 2008. Angiopoietin-1 and -2 expression in recurrent squamous cell carcinoma of the oral cavity. J. Surg. Oncol. 97 (3), 273–277. https://doi.org/10.1002/(ISSN)1096-909810.1002/jso.v97:310.1002/jso.20930.

Costa Svedman, F., Pillas, D., Kaur, M., Linder, R., Hansson, J., Aliki, T., 2016. Stage-specific survival and recurrence in patients with cutaneous malignant melanoma in Europe: a systematic review of the literature. Clin. Epidemiol. 109. https://doi.org/10.2147/CLEP.S99021.

Doğan, A., Demirci, S., Apdik, H., Apdik, E.A., Şahin, F., 2017. Dental pulp stem cells (DPSCs) increase prostate cancer cell proliferation and migration under in vitro conditions. Tissue Cell 49 (6), 711–718. https://doi.org/10.1016/j.tice:2017.10.003.

Dominici, M., Le Blanc, K., Mueller, I., Slaper-Cortenbach, I., Marini, F.C., Krause, D.S., Deans, R.J., Keating, A., Prockop, D.J., Horwitz, E.M., 2006. Minimal criteria for defining multipotent mesenchymal stromal cells. the international society for cellular therapy position statement. Cytotherapy 8 (4), 315–317. https://doi.org/10.1080/14653240600855905.

Elahi, M., Rakhshan, V., 2020. MED15, transforming growth factor beta 1 (TGF-β1), FcγRIII (CD16), and HNK-1 (CD57) are prognostic biomarkers of oral squamous cell carcinoma. Sci. Rep. 10, 8475. https://doi.org/10.1038/s41598-020-65145-3.

González-González, L., González-Ramírez, R., Flores, A., Avelino-Cruz, J.E., Felix, R., Monjaraz, E., 2019. Epidermal growth factor potentiates migration of MDA-MB 231 breast cancer cells by increasing NaV1.5 channel expression. Oncology 97, 373–382. https://doi.org/10.1159/000501802.

Gunawardena, T.N.A., Rahman, M.T., Abdullah, B.J.J., Abu Kasim, N.H., 2019. Conditioned media derived from mesenchymal stem cell cultures: the next generation for regenerative medicine. J. Tissue Eng. Regen. Med. 13 (4), 569–586. https://doi.org/10.1002/term.v13.410.1002/term.2806.

Guo, X.Y., Zhang, J.Y., Shi, X.Z., Wang, Q., Shen, W.L., Zhu, W.W., Liu, L.K., 2020. Upregulation of CSF-1 is correlated with elevated TAM infiltration and poor prognosis in oral squamous cell carcinoma. Am. J. Transl. Res. 12, 6235–6249.

Hollmén, M., Karaman, S., Schwager, S., Lisibach, A., Christiansen, A.J., Maksimow, M., Varga, Z., Jalkanen, S., Detmar, M., 2016. G-CSF regulates macrophage phenotype and associates with poor overall survival in human triple-negative breast cancer. Oncoimmunology 5 (3), e1115177. https://doi.org/10.1080/2162402X.2015.1115177.

Horwitz, E.M., Le Blanc, K., Dominici, M., Mueller, I., Slaper-Cortenbach, I., Marini, F. C., Deans, R.J., Krause, D.S., Keating, A., 2005. Clarification of the nomenclature for MSC: the international society for cellular therapy position statement. Cytotherapy 7 (5), 393–395. https://doi.org/10.1080/14653240500319234.

Hussein, M.Z., Al Fikky, A., Abdel Bar, I., Attia, O., 2004. Serum IL-6 and IL-12 levels in breast cancer patients. Egypt. J. Immunol. 11, 165–170.

Irastorza, I., Luzuriaga, J., Martinez-Conde, R., Ibarretxe, G., Unda, F., 2019. Adhesion, integration and osteogenesis of human dental pulp stem cells on biomimetic implant surfaces combined with plasma derived products. Eur. Cells Mater. 38, 201–214. https://doi.org/10.22203/eCM.v038a14.

Iwanaka, T., Yamaza, T., Sonoda, S., Yoshimaru, K., Matsuura, T., Yamaza, H., Ohga, S., Oda, Y., Taguchi, T., 2020. A model study for the manufacture and validation of clinical-grade deciduous dental pulp stem cells for chronic liver fibrosis treatment. Stem Cell Res. Ther. 11, 134. https://doi.org/10.1186/s13287-020-01630-w.

Ji, X., Zhang, Z., Han, Y., Song, J., Xu, X., Jin, J., Su, S., Mu, D., Liu, X., Xu, S., Cui, H., Zhao, Z., Wang, Y., Liu, H., 2016. Mesenchymal stem cells derived from normal gingival tissue inhibit the proliferation of oral cancer cells in vitro and in vivo. Int. J. Oncol. 49, 2011–2022. https://doi.org/10.3892/ijo.2016.3715.

Jin, W., Lin, Z., Zhang, X., Kong, L., Yang, L.i., 2015. Effects and mechanism of recombinant human erythropoietin on the growth of human breast cancer MDA-MB-231 cells in nude mice. Pathol. - Res. Pract. 211 (8), 570–576. https://doi.org/10.1016/j.prp.2015.04.006.

Kheur, S., Sanap, A., Kharat, A., Gupta, A.A., Raj, A.T., Kheur, M., Bhonde, R., 2020. Hypothesizing the therapeutic potential of mesenchymal stem cells in oral submucous fibrosis. Med. Hypotheses 144, 110204. https://doi.org/10.1016/j.mehy.2020.110204.

Krasagakis, K., Garbe, C., Zouboulis, C.C., Orfanos, C.E., 1995. Growth Control of Melanoma Cells and Melanocytes by Cytokines. pp. 169–182. https://doi.org/10.1007/978-3-642-78771-3_12

Kuang, W., Deng, Q., Deng, C., Li, W., Shu, S., Zhou, M., 2017. Hepatocyte growth factor induces breast cancer cell invasion via the PI3K/Akt and p38 MAPK signaling pathways to up-regulate the expression of COX2. Am. J. Transl. Res. 9, 3816–3826.

L., P.K., Kandoi, S., Misra, R., S., V., K., R., Verma, R.S., 2019. The mesenchymal stem cell secretome: a new paradigm towards cell-free therapeutic mode in regenerative medicine. Cytokine Growth Factor Rev. 46, 1–9. https://doi.org/10.1016/j.cytogfr.2019.04.002.

Lenze, N.R., Farquhar, D.R., Dorismond, C., Sheth, S., Zevallos, J.P., Blumberg, J., Lumley, C., Patel, S., Hackman, T., Weissler, M.C., Yarbrough, W.G., Olshan, A.F., Zanation, A.M., 2020. Age and risk of recurrence in oral tongue squamous cell carcinoma: Systematic review. Head Neck 42 (12), 3755–3768. https://doi.org/10.1002/hed.v42.1210.1002/hed.26464.

Li, C., Sun, C., Fan, J., Geng, N., Li, C.-H., Liao, J., Mi, K., Zhu, G., Ma, H., Song, Y., Tang, Y., Chen, Y., 2013. Angiopoietin-2 expression is correlated with angiogenesis and overall survival in oral squamous cell carcinoma. Med. Oncol. 30, 571. https://doi.org/10.1007/s12032-013-0571-2.

Li, J., Liu, J., Mao, X., Tang, Q., Lu, H., 2014. IL-7 Receptor Blockade Inhibits IL-17-Producing γδ Cells and Suppresses Melanoma Development. Inflammation 37 (5), 1444–1452. https://doi.org/10.1007/s10753-014-9869-2.

Lin, J.-S., Sun, F.-J., Lin, P.-Y., Chang, K.-W., Yang, C.-C., Liu, C.-J., 2018. Clinicopathological and prognostic significance of preoperative serum epidermal growth factor levels in patients with oral squamous cell carcinoma. Int. J. Oral Maxillofac. Surg. 47 (10), 1236–1242. https://doi.org/10.1016/j.ijom.2018.01.023.

Lin, L.-H., Lin, J.-S., Yang, C.-C., Cheng, H.-W., Chang, K.-W., Liu, C.-J., 2020. Overexpression of platelet-derived growth factor and its receptor are correlated with oral tumorigenesis and poor prognosis in oral squamous cell carcinoma. Int. J. Mol. Sci. 21, 2360. https://doi.org/10.3390/ijms21072360.

Ma, Y., Ren, Y., Dai, Z.-J., Wu, C.-J., Ji, Y.-H., Xu, J., 2017. IL-6, IL-8 and TNF-α levels correlate with disease stage in breast cancer patients. Adv. Clin. Exp. Med. 26, 421–426. https://doi.org/10.17219/acem/62120.

Marofi, F., Vahedi, G., Biglari, A., Esmaeilzadeh, A., Athari, S.S., 2017. Mesenchymal stromal/stem cells: a new era in the cell-based targeted gene therapy of cancer. Front. Immunol. 8. https://doi.org/10.3389/fimmu.2017.01770.

Nakajima, K., Kunimatsu, R., Ando, K., Ando, T., Hayashi, Y., Kihara, T., Hiraki, T., Tsuka, Y., Abe, T., Kaku, M., Nikawa, H., Takata, T., Tanne, K., Tanimoto, K., 2018. Comparison of the bone regeneration ability between stem cells from human exfoliated deciduous teeth, human dental pulp stem cells and human bone marrow mesenchymal stem cells. Biochem. Biophys. Res. Commun. 497 (3), 876–882. https://doi.org/10.1016/j.bbrc.2018.02.156.

Obayashi-Ishii, M., Saito, S., Omagari, D., Asano, M., Ishigami, T., 2018. A static magnetic field inhibits the expression of platelet-derived growth factor-AA in human oral squamous cell carcinoma. J. Oral Sci. 60 (3), 374–380. https://doi.org/10.2334/josnusd.17-0380.

Patil, V.R., Kharat, A.H., Kulkarni, D.G., Kheur, S.M., Bhonde, R.R., 2018. Long term explant culture for harvesting homogeneous population of human dental pulp stem cells. Cell Biol. Int. 42, 1602–1610. https://doi.org/10.1002/cbin.11065.

Pérez-González, O., Cuéllar-Guzmán, L.F., Soliz, J., Cata, J.P., 2017. Impact of regional anesthesia on recurrence, metastasis, and immune response in breast cancer surgery. Reg. Anesth. Pain Med. 42 (6), 751–756. https://doi.org/10.1097/AAP.0000000000000662.

Qiu, Y.-F., Wang, M.-X., Meng, L.-N., Zhang, R., Wang, W., 2018. MiR-21 regulates proliferation and apoptosis of oral cancer cells through TNF-α. Eur. Rev. Med. Pharmacol. Sci. 22, 7735–7741. https://doi.org/10.26355/eurrev_201811_16395.

Raj, A.T., Kheur, S., Bhonde, R., Gupta, A.A., Patil, S., 2021. Assessing the effect of human mesenchymal stem cell-derived conditioned media on human cancer cell lines: a systematic review. Tissue Cell 71, 101505. https://doi.org/10.1016/j.tice:2021.101505.

Rajaee, A., Sadr-Eshkevari, P., McMasters, K.M., Egger, M.E., 2021. Predictors of nonsentinel lymph node metastasis in cutaneous melanoma: a systematic review and meta-analysis. J. Surg. Res. 260, 506–515. https://doi.org/10.1016/j.jss.2020.11.058.

Richardsen, E., Uglehus, R.D., Johnsen, S.H., Busund, L.-T., 2015. Macrophage-colony stimulating factor (CSF1) predicts breast cancer progression and mortality. Anticancer Res. 35, 865–874.

Rossi, S., Cordella, M., Tabolacci, C., Nassa, G., D'Arcangelo, D., Senatore, C., Pagnotto, P., Magliozzi, R., Salvati, A., Weisz, A., Facchiano, A., Facchiano, F., 2018. TNF-alpha and metalloproteases as key players in melanoma cells aggressiveness. J. Exp. Clin. Cancer Res. 37, 326. https://doi.org/10.1186/s13046-018-0982-1.

Sung, H., Ferlay, J., Siegel, R.L., Laversanne, M., Soerjomataram, I., Jemal, A., Bray, F., 2021. Global cancer statistics 2020: GLOBOCAN estimates of incidence and mortality worldwide for 36 cancers in 185 countries. CA. Cancer J. Clin. 71 (3), 209–249. https://doi.org/10.3322/caac.v71.310.3322/caac.21660.

The Economic Burden of Cancer | The Cancer Atlas [WWW Document], n.d. URL https://canceratlas.cancer.org/taking-action/economic-burden/ (accessed 4.29.21).

Wang, X., Wang, N., Zhong, L., Wang, S., Zheng, Y., Yang, B., Zhang, J., Lin, Y.i., Wang, Z., 2020. Prognostic value of depression and anxiety on breast cancer recurrence and mortality: a systematic review and meta-analysis of 282,203 patients. Mol. Psychiatry 25 (12), 3186–3197. https://doi.org/10.1038/s41380-020-00865-6.

Warshavsky, A., Rosen, R., Nard-Carmel, N., Abu-Ghanem, S., Oestreicher-Kedem, Y., Abergel, A., Fliss, D.M., Horowitz, G., 2019. Assessment of the Rate of Skip Metastasis to Neck Level IV in Patients With Clinically Node-Negative Neck Oral Cavity Squamous Cell Carcinoma. JAMA Otolaryngol. Neck Surg. 145 (6), 542. https://doi.org/10.1001/jamaoto.2019.0784.

Wu, X., Sun, A., Yu, W., Hong, C., Liu, Z., 2020. CXCL10 mediates breast cancer tamoxifen resistance and promotes estrogen-dependent and independent proliferation. Mol. Cell. Endocrinol. 512, 110866. https://doi.org/10.1016/j.mce:2020.110866.

Yu, G., Zhou, A., Xue, J., Huang, C., Zhang, X., Kang, S.-H., Chiu, W.-T., Tan, C., Xie, K., Wang, J., Huang, S., 2015. FoxM1 promotes breast tumorigenesis by activating PDGF-A and forming a positive feedback loop with the PDGF/AKT signaling pathway. Oncotarget 6, 11281–11294. https://doi.org/10.18632/oncotarget.3596.

Zanoni, D.K., Montero, P.H., Migliacci, J.C., Shah, J.P., Wong, R.J., Ganly, I., Patel, S.G., 2019. Survival outcomes after treatment of cancer of the oral cavity (1985–2015). Oral Oncol. 90, 115–121. https://doi.org/10.1016/j.oraloncology.2019.02.001.